# Design and Performances of a 200 Mbit/s 16 QAM Digital Radio System

IZUMI HORIKAWA, TAKEHIRO MURASE, AND YOICHI SAITO

*Abstract*—**A novel long haul 5 GHz 16 QAM digital radio system, which has 200 Mbit/s transmission capacity within the 40 MHz interleaved channel allocation, is proposed and described. It is designed to be overbuilt on existing FDM-FM routes with an approximately 50 km repeater spacing. To achieve the 5 bit/s/Hz RF spectral efficiency, the 16 QAM modulation and Nyquist cosine roll-off spectral shaping techniques ($\alpha = 0.5$) are investigated. Then a new signal shaping filter, differential encoding and carrier recovery techniques are presented. Finally, the effects of TWT amplifier nonlinearity on a 16 QAM signal are experimentally investigated.**

## I. INTRODUCTION

"DIGITAL Radio" is an attractive transmission system in digitalizing a communication network. In designing a microwave digital ratio system as a large capacity trunk transmission system, particular consideration should be taken of the efficient use of the radio frequency spectrum, and of the compatibility with existing analog FM systems, such as transmission capacity, frequency allocation, repeater spacing, repeater station facilities, etc. Several digital radio systems have already been developed or are now being investigated in the microwave frequency band [1]-[6]. They employ the 4, 8 PSK or QPRS modulation techniques with around 4 bit/s/Hz RF spectral efficiency. Transmission capacities are less than 100 Mbits/s, except for systems in 18-20 GHz bands [5], [6].

In this paper, a novel long haul 5 GHz 16 QAM digital radio system, which has 200 Mbit/s transmission capacity within the 40 MHz interleaved channel allocation, is proposed and its system design considerations as well as the hardware performances are described. This system is designed to be overbuilt on existing FDM-FM routes with approximately 50 km repeater spacing.

To achieve the 5 bit/s/Hz RF spectral efficiency, the following three important tasks have to be completed.

(1) The developing of a 200 Mbit/s capacity system design within the 40 MHz bandwidth.

(2) The developing of 16 QAM modulation/demodulation and Nyquist cosine roll-off spectral shaping techniques.

(3) The investigation of multipath fading effects on a multilevel modulated signal and of its countermeasure techniques.

Specifically, the following problems are discussed, which are essential to the realization of this high capacity, high efficiency system.

Manuscript received January 16, 1979; revised June 29, 1979. This paper was presented at the International Conference on Communications, Boston, MA, June 1979.

The authors are with the Yokosuka Electrical Communication Laboratory, Nippon Telegraph and Telephone Public Corporation, Yokosuka-shi, Kanagawa 238-03, Japan.

(1) Modulation technique. (2) Simple differential encoding for multilevel QAM systems. (3) New binary transversal filters. (4) Carrier recovery with selective gated PLL. Finally, the effects of TWT amplifier nonlinearity on a 16 QAM signal are reported.

## II. SYSTEM DESIGN

### A. Modulation Technique

To obtain competitive transmission capacity with large capacity FM systems, a 200 Mbit/s bit rate is needed for the digital systems, which is equivalent to 2880 voice channels. This implies that a highly spectral efficient modulation technique, higher than 2.5 bits/Hz, would have to be developed.

This efficiency can be achieved by multilevel modulation with the Nyquist spectral shaping technique. The conventional 8 PSK with 76 Mbaud symbol rate and rolloff factor $\alpha$ of 0.2 might be one of the possible modulating schemes. However, severe Nyquist transmission, such as $\alpha = 0.2$, is quite sensitive to many kinds of distortions. Besides, the power spillover into the out of guard band in the existing analog system frequency allocations exceeds 1% of the total transmission power. These considerations lead to the 16 level modulation schemes, $\alpha = 0.5$.

The QAM signal constellation is very close to the best performance achievable by the optimum packing of the 16 signal points into two dimensions [7], [8]. Also, the QAM technique is quite suitable for a 200 Mbit/s digital microwave system, taking into account the easy implementation of high speed MODEM circuitry.

### B. System Configuration

Figure 1 and Table 1 show a functional block diagram and system parameters for the 200 Mbit/s 16 QAM digital radio system. The system is composed of three functional blocks: terminal interface, 16 QAM MODEM and radio equipment.

The transmitting terminal interface translates two 100 Mbit/s AMI signals into four 50 Mbit/s NRZ signals. In addition, the terminal interface provides redundunt pulse insertion for monitoring errors, scrambling and differential encoding.

The 16 QAM MODEM is regenerative equipment that carries 200 Mbits/s in a 40 MHz bandwidth at 140 MHz carrier frequency. In order to conserve the 200 Mbit/s signal within 40 MHz, the 16 QAM modulation and the Nyquist channel ($\alpha = 0.5$) techniques are used. The transmitting and receiving filters are adopted at the baseband, since two dimensional modulation systems, such as 8 PSK, QPRS or 16 QAM, are sensitive to asymmetrical transmission responses, and since it is difficult to realize the accurate required filter at IF or RF.

0090-6778/79/1200-1953$00.75 

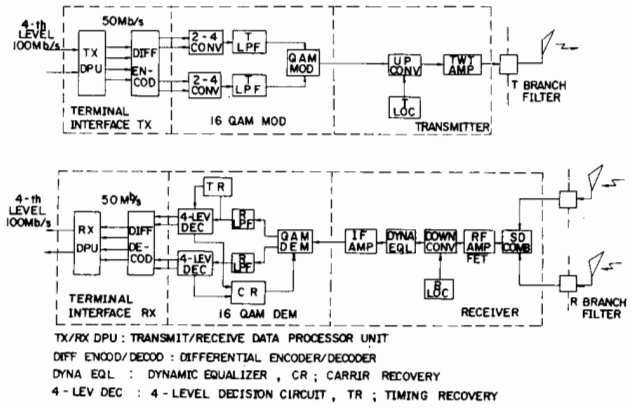


Fig. 1 Block diagram of 16 QAM system.

TABLE 1
200 Mbit/s 16 QAM DIGITAL RADIO SYSTEM PARAMETERS

| | |
|---|---|
| Frequency band | 4.4 ~ 5.0 GHz |
| Capacity | 200 Mbit/s. sys |
| Modulation | 16 QAM |
| Demodulation | Coherent detection |
| Symbol rate | 50 MB |
| RF channel spacing | 40 MHz |
| Repeater spacing | 50 km |
| Regeneration | Every repeater |

The radio equipment has almost the same functions as those of high capacity FM systems. In addition, the receiver is equipped with an equal-gain in-phase combiner and a dynamic equalizer to improve frequency distortion caused by selective fading.

## III. CIRCUIT DESCRIPTION

### A. Differential Encoding for Multiple QAM systems

A problem arises at the demodulator in the practical hardware design phase. This results from the fact that the demodulator can recognize the pattern of signal points but cannot distinguish between the various symmetric phase orientations of the signal set. This ambiguity has to be resolved in some way. The use of differential encoding has the advantages of no redundunt information insertion and easy implementation.

The rectangular signal sets in two-dimension are, generally, constructed from two $2-2^M$ level converters and a quadrature amplitude modulator. Another new technique, which generates the signal sets by summing the outputs of two multiphase modulators, has been recently proposed [9]. Generalizing these two generating techniques and considering the relations between the two methods, a simple differential encoding for multilevel signal sets can be derived. Figure 2 illustrates the relation between the QAM technique and the new "superimposed modulation" technique for $2^M \times 2^M$ rectangular signal sets. As illustrated in Fig. 2, the pair of $i$-th figure digital signals, at the $2-2^M$ level converter $2^{i-1}b_{xi}$ and $2^{i-1}b_{yi}$, is equivalent to the 4PSK signal $(4\text{PSK})^{i-1}$.

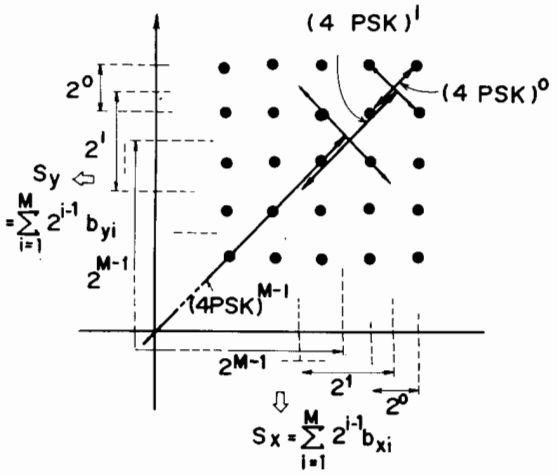


Fig. 2 Relation on $2^M \times 2^M$ rectangular signal set between $2^M \times 2^M$ level converter output signals and 4 PSK signals.

From these discussions, it becomes clear that the $i$-th figure signals of D/A converter output are the same as the figure signals of the $2^M$-level decision circuit at the demodulator, and also that each pair of the same figure signals forms individual 4 PSK signals.

Therefore, the differential encoder and decoder for $2^M \times 2^M$ QAM systems can be implemented with $M$ pairs of module-4 summing and subtracting logic circuits by processing the latter with their $i$-th figure signals in pairs of D/A and A/D converter output, as shown in Fig. 3. These differential encoding and decoding logic equations are shown Eq. (1).

Encoder

$$Y_i^n(b_{xi}^n, b_{yi}^n) = X_i^n(a_{xi}^n, a_{yi}^n) \oplus Y_i^{n-l}(b_{xi}^{n-l}, b_{yi}^{n-l}) \quad \text{mod} - 4 \tag{1}$$

Decoder

$$X_i^n(a_{xi}^n, a_{yi}^n) = Z_i^n(c_{xi}^n, c_{yi}^n) \ominus Z_i^{n-l}(c_{xi}^{n-l}, c_{yi}^{n-l}) \quad \text{mod} - 4$$

where $X_i^n(a_{xi}^n, a_{yi}^n)$, $Y_i^n(b_{xi}^n, b_{yi}^n)$ and $Z_i^n(c_{xi}^n, c_{yi}^n)$ express their quaternary numbers, which consist of each pair of binary signals, $a_{xi}^n$, $a_{yi}^n$, etc.

Using this coding procedure along with the encoding for PSK systems, the bit error is increased twofold. This corresponds to 0.3 dB $C/N$ degradation. However, the difference in $C/N$ degradation between this procedure and another possible procedure [10] is only 0.1 dB.

Thus, the differential encoding procedure for multilevel QAM signals is quite simple, and the implementation of the encoding scheme can easily be constructed by adopting the same logic circuitry.

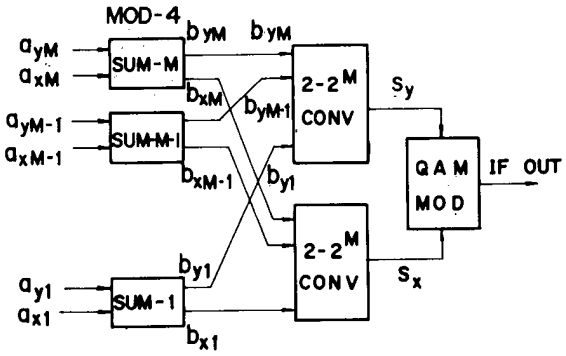


Fig. 3 Differential encoding for $2^M \times 2^M$ QAM.

### B. Binary Transversal Filters

The transmitting spectral shaping filter controls the overall transmission characteristic for the Nyquist channel. Binary transversal filters (BTF's) are effective for accurate spectral shaping, since the BTF's directly generate the required waveform through the design procedure of the time domain. This section describes the new design principle for the binary transversal filter (BTF).

A conventional BTF [11], [12] processing a return-to-zero type pulse stream has to be equipped with an NRZ-RZ converter. As a result, the timing margin decreases, and the discrete frequency component at the symbol rate increases.

This new BTF accepts an NRZ pulse stream without an RZ signal processing stage, as shown in Fig. 4. NRZ pulses of width "$T$," generally, can be considered as $L$ RZ pulses of width "$T/L$", superposed in the time difference of $T/L$, where $L$ is an integer.

This means that this new BTF is equivalent to combining the $L$ conventional BTF with the time difference of $T/L$. From these facts, the following equations are given in both time and frequency domain.

For $L = 2K$

$$a(t) = \sum_{k=1}^{K} \left\{ s\left[t - \frac{2k+1}{2K} \cdot \frac{T}{2}\right] + s\left[t + \frac{2k+1}{2K} \cdot \frac{T}{2}\right] \right\}$$

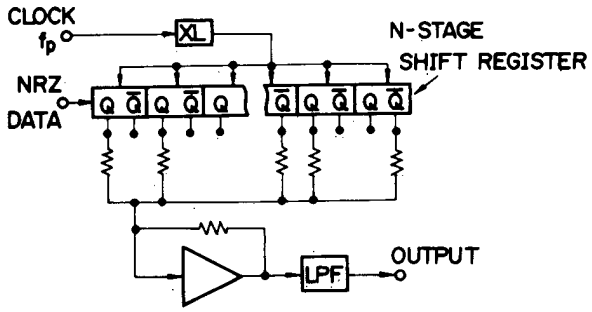


Fig. 4 Binary transversal filter.

$$A(f) = 2S(f) \sum_{k=1}^{K} \left\{ \cos\left[\frac{2k+1}{2K} \pi f T\right] \right\} \tag{2}$$

$$= S(f) \cdot H_{2K}(f). \tag{3}$$

And, for $L = 2K + 1$,

$$a(t) = s(t) + \sum_{k=1}^{K} \left\{ s\left(t - \frac{2k}{2K+1} \cdot \frac{T}{2}\right) + s\left(t - \frac{2k}{2K+1} \cdot \frac{T}{2}\right) \right\}. \tag{4}$$

$$A(f) = S(f) \left[1 + 2 \sum_{k=1}^{K} \cos\left(\frac{2k}{2K+1} \pi f T\right)\right]$$

$$= S(f) \cdot H_{2K+1}(f) \tag{5}$$

where $s(t)$ is the conventional BTF output signal and $S(f)$ is its Fourier transform. Figure 5 illustrates these relations for $L = 2$. Thus, the new BTF, which accepts an NRZ pulse stream, has the same effect as the conventional BTF's transmission function $H_{2k}(f)$, or $H_{2k+1}(f)$. Therefore, with this new BTF, the expected transmitting spectral $S(f)$ can be designed by substituting $S(f)/H_{2k}(f)$ or, $S(f)/H_{2k+1}(f)$ for $S(f)$ in the conventional BTF design method.

The number of stages of shift register is determined by considering the residual intersymbol interference, out of band energy and circuit size. The eleven stage shift registers are selected and three MECL 10 K IC's are driven by a 100 MHz clock signal. Figure 6 shows the theoretical and experimental BTF output spectral density for $\alpha = 0.5$. The new BTF generates no discrete symbol frequency component, and effectively reduces the residual out of band energy in the $f/fp = 1.0$ vicinity. The measured spectral performance agrees exactly with the theoretical value. The out of band spectrum was reduced by fifth order Chebyshev LPF of 60 MHz cutoff (0.01 dB ripple). Figure 7 shows eye diagrams of the BTF, comparing it with conventional and new type BTF's. At the LPF output, an accurate Nyquist pulse waveform with less than 3% of intersymbol interference is achieved, and is shown in Fig. 8.

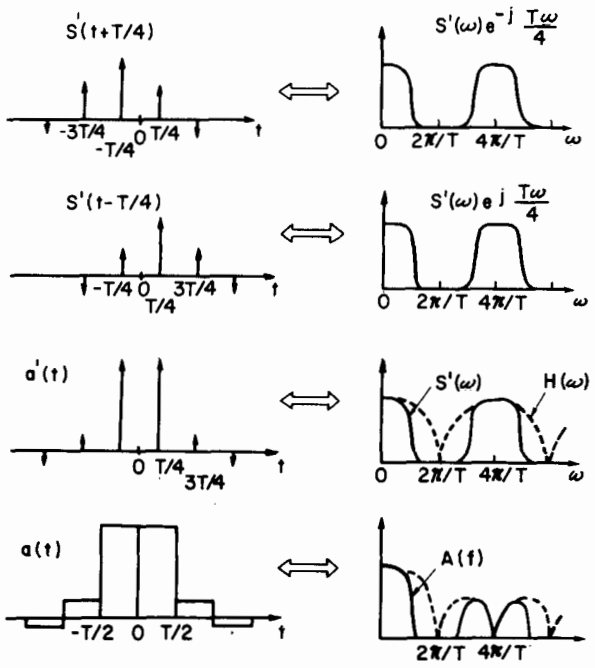


Fig. 5 Waveform and spectral function for new BTF; $L = 2$.

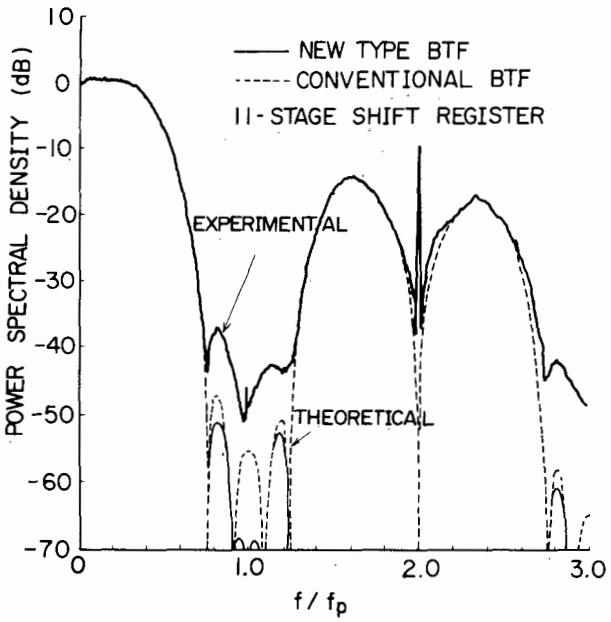


Fig. 6 Measured and calculated power spectral density; $\alpha = 0.5$.

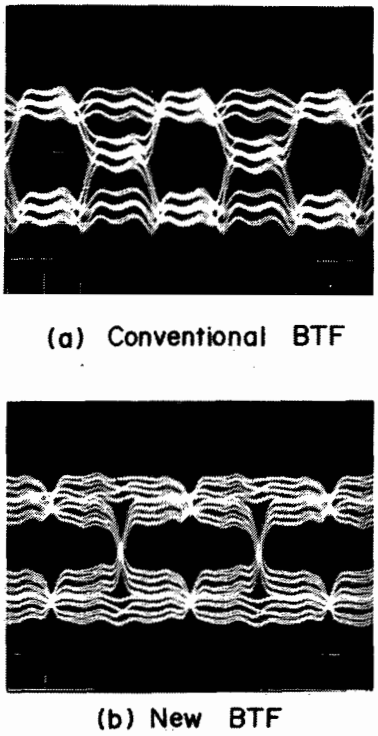


Fig. 7 Eye diagrams of th BTF comparing with conventional and new type BTF's.

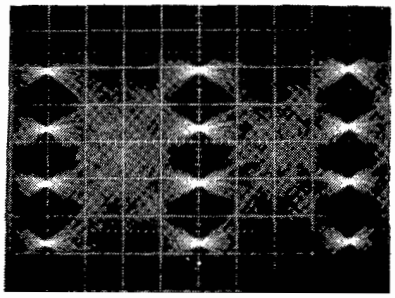

Fig. 8 4-level eye diagram for BTF followed by an LPF, horizontal 5 ns/div.

### C. Carrier Recovery

Highly coherent quadrature references are required for synchronous demodulation of the QAM signal. A number of methods for generating carrier references from a suppressed carrier signal, such as PSK signals, have been established [13]. Similarly, these carrier tracking loops are applicable [14]. However, problems were encountered in the 16 QAM carrier recovery. The carrier tracking loop for the QAM signal has to hold only four stable phase points as well as 4PSK systems, and simultaneously has to have a good phase jitter performance. A novel carrier recovery with a selective gated phase-locked loop (PLL) has been developed for this system. Figure 9 shows a functional block diagram of the carrier recovery circuit for 16 QAM signal.

Half of the 16 QAM signal points is different from the 4 PSK signal phases. This causes undesirable false lock phenomena and a severe phase jitter. Therefore, in this carrier tracking loop, first, an error signal, which is proportional to the phase error between the incoming and the locally generated carrier, is generated by nonlinear processing of 4 PSK signals. Next, the obtained error signal is selectively gated with the control signal, which is driven by a phase recognition circuit. Thus, this loop is controlled by only the error signal derived from the same phases of 4 PSK signal. In this experimental carrier tracking loop, Costas processing with EXCLUSIVE-OR circuits is employed for nonlinear processing, and an ECL Master-Slave Flip Flop is used for a sample and hold circuit.

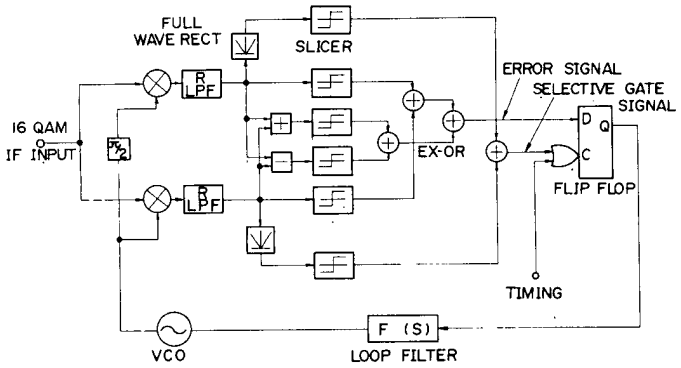


Fig. 9 Block diagram of the carrier recovery with selective gated PLL.

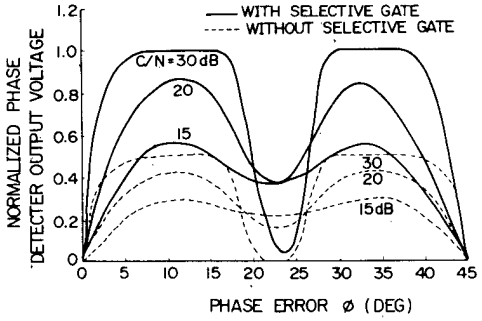


Fig. 10 Equivalent phase detector characteristics of the loop.

Figure 10 shows an equivalent phase detector characteristic of this carrier recovery. Note that the loop exhibits only the desired stable lock point at $\phi = 0$ and, simultaneously, improves detector sensitivity twice as much as the conventional 4 PSK nonlinear processing.

The measured rms carrier jitter is about 0.4 degrees, and the pull-in frequency range is more than ±300 kHz without sweep acquisition in 200 Mbit/s 16 QAM systems.

## IV. ERROR RATE PERFORMANCE

Figure 11 shows the theoretical and experimental error rate performances of a 200 Mbit/s 16 QAM repeater. The 16 QAM MODEM, with about 1.5 dB *C/N* degradation, is achieved as shown in Fig. 11. Main error degradation sources are 1) imperfection of ring modulator and demodulator, 2) residual intersymbol interference due to delay and amplitude distortions, and 3) differential encoding. The difference in *C/N* degradations, between MODEM's back to back and *T-R*'s back to back, is caused by TWT amplifier nonlinearity.

The effects of TWT amplifier nonlinearity for the 16 QAM signal have not been reported. In order to clarify the effects due to the nonlinear distortions (AM-PM conversion and gain deviation), experimental investigations have been carried out.

Two kinds of TWT amplifier with different nonlinear characteristics and saturation power (45 dBm saturation power for LD4217 and 34.5 dBm for LD4007) are used. Figure 12 shows the measured nonlinear characteristics with respect to output back off of TWT's. Note that AM-PM conversions prevail, even in the smaller output power region. For these TWT's, the

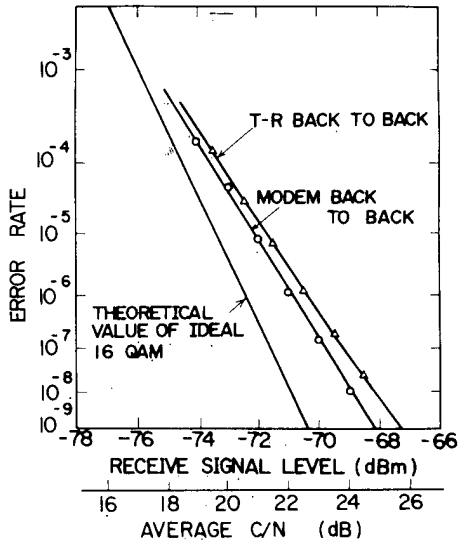


Fig. 11 Bit error rate performances, MODEM back to back and overall repeater back to back.

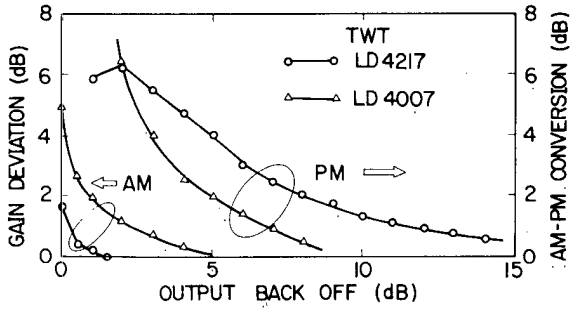


Fig. 12 Two TWT's nonlinear characteristics.

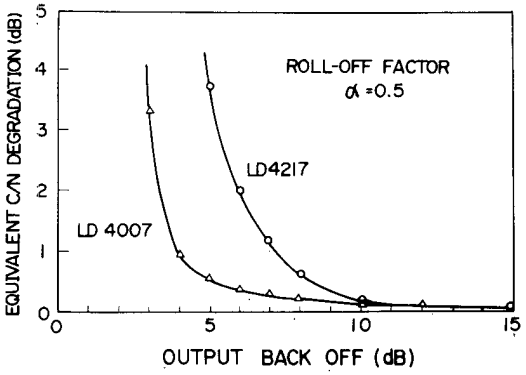


Fig. 13 Equivarent *C/N* degradation due to TWT nonlinearity.

measured equivalent *C/N* degradations are shown in Fig. 13. From Figs. 12 and 13, it is shown that AM-PM conversion mainly dominates the error degradation caused by TWT nonlinearity. From the above results, TWT nonlinear distortions on a 16 QAM signal can be evaluated, and it is concluded that a TWT should be operated at the power level at which the AM-PM conversion is less than 2 deg/dB, in order to suppress *C/N* degradation to less than 0.5 dB.

DOCKET ALARM

# Explore Litigation Insights

Docket Alarm provides insights to develop a more informed litigation strategy and the peace of mind of knowing you're on top of things.

## Real-Time Litigation Alerts

Keep your litigation team up-to-date with **real-time alerts** and advanced team management tools built for the enterprise, all while greatly reducing PACER spend.

Our comprehensive service means we can handle Federal, State, and Administrative courts across the country.

## Advanced Docket Research

With over 230 million records, Docket Alarm's cloud-native docket research platform finds what other services can't. Coverage includes Federal, State, plus PTAB, TTAB, ITC and NLRB decisions, all in one place.

Identify arguments that have been successful in the past with full text, pinpoint searching. Link to case law cited within any court document via Fastcase.

## Analytics At Your Fingertips

Learn what happened the last time a particular judge, opposing counsel or company faced cases similar to yours.

Advanced out-of-the-box PTAB and TTAB analytics are always at your fingertips.

## API

Docket Alarm offers a powerful API (application programming interface) to developers that want to integrate case filings into their apps.

**LAW FIRMS**
Build custom dashboards for your attorneys and clients with live data direct from the court.

Automate many repetitive legal tasks like conflict checks, document management, and marketing.

**FINANCIAL INSTITUTIONS**
Litigation and bankruptcy checks for companies and debtors.

**E-DISCOVERY AND LEGAL VENDORS**
Sync your system to PACER to automate legal marketing.